Journal Name

ARTICLE TYPE

Cite this: DOI: 10.1039/xxxxxxxxxx

Mechanism suppressing charge recombination at iodine defects in $CH_3NH_3PbI_3$ by polaron formation

Julia Wiktor,*[a] Francesco Ambrosio,[a] and Alfredo Pasquarello[a]

Received Date
Accepted Date

DOI: 10.1039/xxxxxxxxxx

www.rsc.org/journalname

Metal-halide perovskites exhibit high efficiencies in photovoltaic applications and low recombination rates, despite the high concentrations of intrinsic defects. We here study the hole trapping at the negative iodine interstitial, which corresponds to the dominating recombination center in $CH_3NH_3PbI_3$. We calculate the free energy profile for the hole trapping at 300 K using the Blue Moon technique based on hybrid functional molecular dynamics. We find that the hole trapping is energetically unfavorable and requires overcoming an energy barrier. This behavior stems from the position of the vertical $(-/0)$ transition level of the iodine defect and the formation of a polaron. Our simulations show that the polaron does not interact with the iodine interstitial and hops through the lattice on a sub-picosecond scale. Our results highlight a mechanism by which the low mononuclear (trap-assisted) recombination rates in $CH_3NH_3PbI_3$ can be explained.

Metal-halide perovskites, such as methylammonium lead iodide ($CH_3NH_3PbI_3$), have emerged as promising materials for high efficiency solar cells.[1–3] One of the main reasons for the outstanding performance of devices based on halide perovskites, is the slow recombination of photogenerated carriers[4–6]. It has been shown that the recombination rates measured in $CH_3NH_3PbI_3$ are dominated by the bimolecular recombination process.[7–9] The very low monomolecular (trap-assisted) recombination rate is surprising, considering that perovskites are generally processed at low temperature,[10–12] which would suggest high concentrations of intrinsic defects. Additionally, using advanced hybrid functional calculations including spin-orbit coupling effects, Du[13] showed that iodine-related defects in $CH_3NH_3PbI_3$, such as iodine interstitials, introduce deep hole and electron trapping levels inside the band gap and should play a role in carrier trapping and recombination.

To understand the low recombination rates at iodine interstitials in $CH_3NH_3PbI_3$, it is necessary to determine their dominating charge state. Experimental studies indicate that single-crystalline samples of $CH_3NH_3PbI_3$ are intrinsic or slightly p-doped,[14] while n-doping is observed in thin films near the surface.[15] According to computational studies,[13,16] the iodine interstitial should be stable in a negative charge state in intrinsic, n-doped and slightly p-doped $CH_3NH_3PbI_3$ samples. Stability of I_i^- can be expected for a wide range of Fermi levels, since such a defect corresponds to simply adding an iodine anion in its formal -1 charge state to the lattice. Meggiolaro *et al.*[16] found that the Fermi level is pinned close to the middle of the band gap in stoichiometric samples. These findings indicate that the negative charge state of the iodine interstitial should be the dominant one in $CH_3NH_3PbI_3$ samples. However, the low recombination rate at this defect state still remains to be clarified. One possible explanation for the low recombination rates at the negatively charged iodine interstitial could be related to kinetic barriers for the charge trapping. Even though the $(0/-)$ thermodynamic transition level of the iodine interstitial is inside the gap of $CH_3NH_3PbI_3$,[16–19] it has been observed that the vertical level for the extraction of an electron from the I_i^- defect lies below the valence band maximum (VBM)[17]. This means that upon excitation of I_i^- an electron is removed from a delocalized valence state and not from the interstitial. The creation of I_i^0 might then involve the overcoming of a kinetic barrier.

We here investigate hole trapping at the iodine interstitial in $CH_3NH_3PbI_3$ and show that polarons might prevent this process. We perform hybrid functional molecular dynamics (MD) simulations of the negatively charged and the neutral iodine interstitial. We find that upon photoexcitation the negatively charged iodine interstitial retains its charge state, while the hole forms a polaron, which is free to hop between the inorganic layers of the perovskite. Our calculations indicate that the trapping of the hole at the defect site is energetically unfavorable and requires overcoming an energy barrier. Consequently, polaron formation suppresses the charge recombination at iodine defects in $CH_3NH_3PbI_3$.

For the monomolecular recombination to occur at the negatively charged iodine interstitial I_i^- (see Fig. 1), an electron-hole pair needs to be first generated, for instance through photoexcitation. Then, the interstitial should trap a hole and create a neutral defect I_i^0. We note that as the vertical $(-/0)$ level is below

[a] *Chaire de Simulation à l'Echelle Atomique (CSEA), Ecole Polytechnique Fédérale de Lausanne (EPFL), CH-1015 Lausanne, Switzerland; E-mail: julia.wiktor@epfl.ch*

VBM[13], this step should correspond to an energy increase, and could therefore involve a kinetic barrier. Next, I_i^0 with the trapped hole would relax to its equilibrium geometry and be ready to capture an electron, acting in this way as a recombination center. When the cycle is completed, the iodine interstitial returns to its negatively charged ground state, which could then serve again as a recombination center. We here study the process of hole trapping at the negatively charged interstitial (steps 2 and 3 in Fig. 1). First, we assess the relative stability of the initial and final system. The initial system corresponds to I_i^- in the presence of a free hole. The final system after charge trapping consists of the neutral defect I_i^0. To account for the rotational degrees of freedom of the organic molecules in $CH_3NH_3PbI_3$ in these two states, we perform molecular dynamics simulations at 300 K.

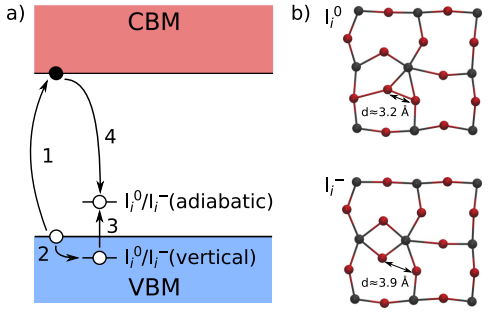

Fig. 1 a) Scheme of the recombination process at the negative iodine interstitial. The following steps are represented: 1) electron-hole pair generation, 2) localization of the hole at the iodine interstitial leading to the change of the charge state, 3) atomic relaxation towards the equilibrium geometry of I_i^0, 4) electron recombination with the trapped hole. b) Representations of the I_i^0 and I_i^- equilibrium structures on the apical site. We only show one plane of Pb and I atoms for clarity.

The calculations presented here are carried out with the CP2K code[20] in the canonical *NVT* ensemble. In the simulations, we describe the orbitals with atom-centered Gaussian-type basis functions and the electron density is re-expanded with an auxiliary plane-wave basis set. We use Goedecker-Teter-Hutter pseudopotentials to account for core-valence interactions.[21] Double-ζ polarized basis sets are used for the wave functions[22] along with a cutoff of 800 Ry for the expansion of the electron density in plane waves. The simulations are performed for a 384-atom supercell with an initial apolar arrangement of the organic cations. We note that during the MD simulation at 300 K, the cations undergo free rotations. Following Lahnsteiner *et al.*,[23] we extract from the autocorrelation function the average reorientation time of the molecule of about 4 ps. We use the experimental lattice parameters of the tetragonal phase of $CH_3NH_3PbI_3$.[24] It has been indicated, both in experimental[25–28] and computational[27,29] studies, that free charges in $CH_3NH_3PbI_3$ form localized polaronic states. Therefore, to properly account for such states, the simulations are carried out with the hybrid functional PBE0.[30] In the simulation we neglect spin-orbit coupling, since the transition level of the negative iodine interstitial relative to the VBM remains essentially unaffected by this effect in $CH_3NH_3PbI_3$.[13]

We perform two molecular dynamics simulations in an overall neutral charge state, one starting with the geometry of I_i^0 and one with the geometry of I_i^-. In the latter, a hole in the valence band is present. In the system containing I_i^- and a hole, we observe the formation of a polaron within the first picosecond of the simulation. In Fig. 2, we show the localization of the extra hole in the two states. For I_i^0, the charge is localized on two iodine atoms forming a dimer with an equilibrium distance of about 3.2 Å. This corresponds to the typical I-I distance in I_2^- and is consistent with previous findings.[16,31] In the case of the I_i^-+polaron system, the extra charge forms a polaron, which hops between the available inorganic layers orthogonal to the tetragonal axis, as in the case of a free polaron.[29] We note that, throughout the simulation, the hole polaron retains its localized state, with the hole density being mostly localized within a single PbI_4 unit. For the negatively charged iodine interstitial, the two apical iodine atoms are separated by about 3.9 Å. We observe that during the 4 ps of simulation the two systems retain their starting configurations, indicating that they both correspond to local minima. During the simulation, we do not observe transitions between the two states, which suggests that they are separated by an energy barrier. To assess the relative stability of the two systems, we first examine the total energy obtained in the respective simulations. However, as can be seen in Fig. 3, in both cases we obtain a broad energy distribution, centered around similar average values. These results indicate that such MD simulations are unable to draw the relative energetics of the two systems.

To accurately study the free energy path between the two configurations and their relative stability at 300 K, we use the Blue Moon technique.[32] In this way, we fully take into account the rotational degrees of freedom and the associated screening of the organic cations. The method consists in performing a set of constrained MD simulations, in which we vary the distance ζ between two apical iodine atoms between 3.2 Å and 4.0 Å. The free energy profile $\Delta F(\zeta)$ can then be obtained from the integration of the forces λ (Lagrange multipliers) acting on the constraint over the reaction coordinate ζ:[33]

$$\Delta F(\zeta) = \int_{\zeta_0}^{\zeta} d\zeta' \langle \lambda \rangle_{\zeta'}, \qquad (1)$$

where ζ_0=3.2 Å, corresponding to the equilibrium I-I distance of I_i^0. The free energy profile obtained through the Blue Moon technique is shown in Fig. 4. For each I-I distance we perform a constrained MD simulation lasting between 3.5 to 5 ps. We include error bars estimated through a blocking analysis.[34]

From the free energy profile, we observe that the system in which the negative iodine interstitial retains its charge state and the photogenerated hole forms a free polaron is by 33 meV more stable than the neutral defect. This means that hole trapping at the iodine interstitial in energetically unfavorable. In addition, the capture of a hole by the interstitial requires overcoming a barrier of about 73 meV. While such energies are at the limit of the accuracy of the methods used, an interesting mechanism nevertheless emerges. The reported barrier is relatively small, and could easily be overcome at room temperature, provided that the polaron remains in the proximity of the interstitial for a signifi-

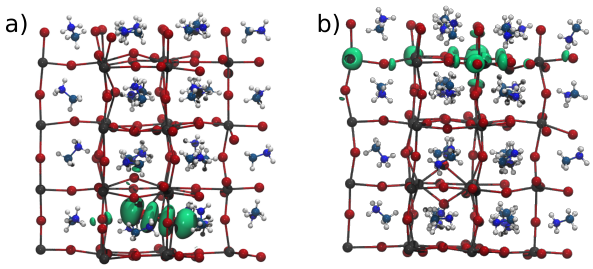

Fig. 2 Isodensities (in green) of the lowest unoccupied state for (a) the neutral iodine interstitial I_i^0 and (b) the system containing a negatively charged interstitial I_i^- and a hole polaron.

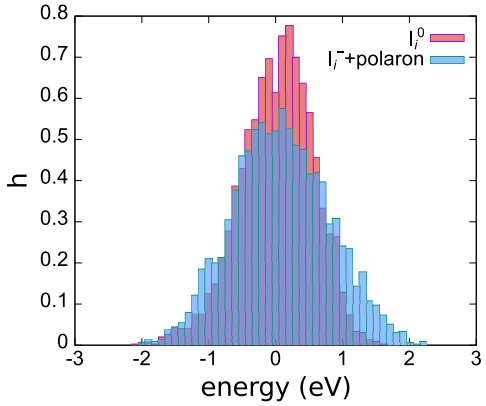

Fig. 3 Histograms of the instantaneous total energy in the simulations of the neutral iodine interstitial I_i^0 and the system containing a negatively charged interstitial I_i^- and a hole polaron. The energy scale is referenced with respect to the average total energy.

cant amount of time. To examine whether the hole polaron remains bound to the iodine interstitial, we monitor its localization during the MD simulation. In Fig. 5, we show the position of the polaron as a function of time. We observe that during the 4 ps of the simulation, the hole hops freely between the inorganic planes orthogonal to the tetragonal axis on a sub-picosecond timescale. This suggests that the kinetic barrier for hole polaron hopping is significantly smaller than kT at room temperature. We note that the polaron hopping is significantly faster that the reorientation of the molecules, which occurs on a picosecond timescale. This is consistent with experimental[28] and computational[29] observations that polaron formation is mostly independent on the cation dynamics in halide perovskites. Would the polaron be efficiently attracted to the negative interstitial lying close to the plane $2z$, the probability of finding the hole density in its proximity (layers $1z$, $2z$ and $3z$) would be higher than for the farthest layer ($4z$). We observe that the polaron is distributed homogeneously across the supercell, suggesting that the negative interstitial is unable to attract the hole polaron. We attribute the suppression of the Coulomb attraction between the two opposite charges to the large static screening in $CH_3NH_3PbI_3$. The order of magnitude of the effective electrostatic interaction between the negative and positive charges can be estimated considering the exciton binding energy in $CH_3NH_3PbI_3$. At room temperature, a binding energy

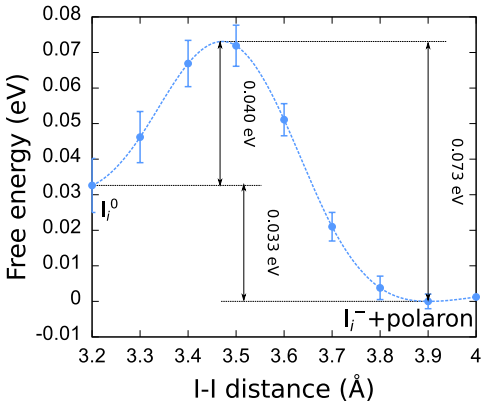

Fig. 4 Free energy profile between the neutral iodine interstitial I_i^0 and the system containing a negative interstitial I_i^- and a hole polaron. The free energy scale is referenced with respect to the minimum energy. The dashed line corresponds to a fit.

of a few millielectronvolts has been measured,[35] in a frequency regime where the effective dielectric constant was estimated to be $\varepsilon \approx 9$. In the static case, in which the dielectric constant amounts to ≈ 70[36], this electrostatic interaction would be further reduced by an order of magnitude. Such an energy is negligible compared to the hole polaron binding energy, which amounts to 90 meV[29]. This explains the absence of any effective binding between the interstitial and the hole, as observed in the simulation. Therefore, we conclude that the hole trapping at the iodine interstitial should have a low probability. First, this is because the hole polaron hops freely through the material and only spends a short time in the close proximity of the well-screened iodine interstitial I_i^-. Second, the phase space associated with the free polaron configurations is much larger than that corresponding to the hole localization on the iodine interstitial, thereby further reducing the probability of trapping.

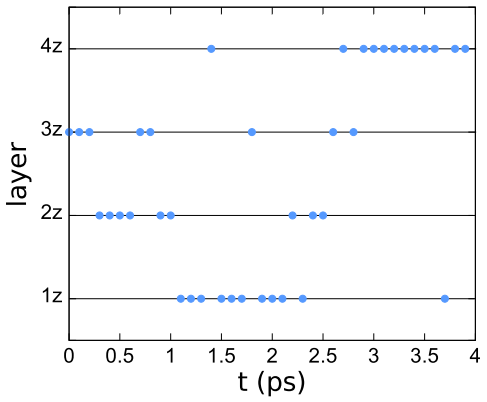

Fig. 5 Hopping of the hole polaron in the presence of a negatively charged iodine interstitial I_i^- during the molecular dynamics. The simulation cell contains four inorganic sublattices orthogonal to the tetragonal axis. The interstitial is centered around the layer $2z$.

We note that we expect a similar behavior for electron trapping at the positively charged state of the iodine interstitial I_i^+. An accurate study of such process would require the inclusion of

spin-orbit coupling, as the conduction band is more strongly affected than the valence band.[13,37] However, combining relativistic calculations with molecular dynamics at the hybrid functional level is at present computationally prohibitive. Nevertheless, we remark that the suppression of hole trapping at I_i^- highlighted here results from the combination of three physical phenomena, which will also occur in the case of electron trapping at the positively charged defect. First, the kinetic energy barrier for charge trapping is due to the fact that the vertical level for electron extraction from I_i^- lies outside the band gap (see Fig. 1). For I_i^+, the vertical level for electron capture also lies outside the band gap, namely within the conduction band.[13] Second, the polaron formation stabilizes the hole and contributes to disfavoring the neutral interstitial. It has previously been shown that the electron, which could be trapped by I_i^+, also forms a polaron on a sub-picosecond timescale[28,29] and should lead to a similar behavior as the one described here for the hole. Third, the probability of hole trapping is reduced due to the efficient static screening of charges in $CH_3NH_3PbI_3$, which will also hold for the electron and the I_i^+ defect.

We note that our results differ from the recent study of Meggiolaro *et al.*[16] on iodine defects. They have found that the negatively charged iodine interstitial traps holes without any barrier when transforming into I_i^0. Then, the trapped hole can recombine with a free electron rapidly. Therefore, Ref. 16 concludes that I_i^- is a potentially harmful defect. However, the study of Meggiolaro *et al.* does not take into account the formation of polarons nor the rotational degrees of freedom of the organic cations, which play a critical role in our model. In the case of the positively charged iodine interstitial, Meggiolaro *et al.* found that the electrons are trapped by I_i^+ without any kinetic barrier. The absence of the barrier is possibly due to the omission of spin-orbit effects in the structural relaxations, as the (+/0) vertical level of the iodine interstitial lies within the conduction band only when these effects are accounted for. In Ref. 16, it is then suggested that the trapped electrons cannot escape the I_i^0 defects immediately, due to the relaxation to a secondary minimum. The long recombination times are thus due to long-living excited defect states, at variance with our model in which the charges are unlikely to be trapped. Charge trapping at the iodine defect has also been studied by Li *et al.*[38]. However, their work focuses on the neutral I_i^0 interstitial, which is a metastable state of this defect,[13] and its interaction with free charges. Therefore, it cannot be directly compared with the present study focusing on the equilibrum charge state of the iodine interstitial, I_i^-.

Our study discloses a mechanism underlying the low recombination rates observed experimentally at defects in halide perovskites and demonstrates the critical role of polarons in this class of materials. We investigated the hole trapping mechanism at the negative iodine interstitial in $CH_3NH_3PbI_3$. We found that it is energetically favorable for the interstitial to retain its negative charge state, while the hole forms a free polaron. Trapping the hole at the interstitial corresponds to a higher free energy and requires overcoming a barrier. Additionally, we showed that the hole polaron freely hops through the $CH_3NH_3PbI_3$ lattice on a sub-picosecond timescale, which further prevents hole trapping. Hence, our study reveals how the mononuclear recombination channel can be suppressed, thereby providing an explanation for the defect-tolerance of halide perovskites.

Conflicts of interest

There are no conflicts to declare.

Acknowledgements

The authors acknowledge financial support from the Swiss National Science Foundation (SNSF) (Grant No. 200020-172524). This work has been realized in relation to the National Center of Competence in Research (NCCR) "Materials' Revolution: Computational Design and Discovery of Novel Materials (MARVEL)" of the SNSF. We used computational resources of CSCS and SCITAS-EPFL.

Notes and references

1 A. Kojima, K. Teshima, Y. Shirai and T. Miyasaka, *J. Am. Chem. Soc.*, 2009, **131**, 6050–6051.
2 H.-S. Kim, C.-R. Lee, J.-H. Im, K.-B. Lee, T. Moehl, A. Marchioro, S.-J. Moon, R. Humphry-Baker, J.-H. Yum, J. E. Moser *et al.*, *Sci. Rep.*, 2012, **2**, 591.
3 G. Hodes, *Science*, 2013, **342**, 317–318.
4 S. D. Stranks, G. E. Eperon, G. Grancini, C. Menelaou, M. J. Alcocer, T. Leijtens, L. M. Herz, A. Petrozza and H. J. Snaith, *Science*, 2013, **342**, 341–344.
5 C. Wehrenfennig, G. E. Eperon, M. B. Johnston, H. J. Snaith and L. M. Herz, *Adv. Mater.*, 2014, **26**, 1584–1589.
6 Y. Bi, E. M. Hutter, Y. Fang, Q. Dong, J. Huang and T. J. Savenije, *J. Phys. Chem. Lett.*, 2016, **7**, 923–928.
7 M. B. Johnston and L. M. Herz, *Acc. Chem. Res.*, 2015, **49**, 146–154.
8 T. M. Brenner, D. A. Egger, L. Kronik, G. Hodes and D. Cahen, *Nat. Rev. Mater.*, 2016, **1**, 15007.
9 Y. Chen, H. Yi, X. Wu, R. Haroldson, Y. Gartstein, Y. Rodionov, K. Tikhonov, A. Zakhidov, X.-Y. Zhu and V. Podzorov, *Nat. Commun.*, 2016, **7**, 12253.
10 G. Xing, N. Mathews, S. Sun, S. S. Lim, Y. M. Lam, M. Grätzel, S. Mhaisalkar and T. C. Sum, *Science*, 2013, **342**, 344–347.
11 J. M. Ball, M. M. Lee, A. Hey and H. J. Snaith, *Energy Environ. Sci.*, 2013, **6**, 1739–1743.
12 J. You, Z. Hong, Y. M. Yang, Q. Chen, M. Cai, T.-B. Song, C.-C. Chen, S. Lu, Y. Liu, H. Zhou *et al.*, *ACS Nano*, 2014, **8**, 1674–1680.
13 M.-H. Du, *J. Phys. Chem. Lett.*, 2015, **6**, 1461–1466.
14 D. Shi, V. Adinolfi, R. Comin, M. Yuan, E. Alarousu, A. Buin, Y. Chen, S. Hoogland, A. Rothenberger, K. Katsiev *et al.*, *Science*, 2015, **347**, 519–522.
15 G. Sadoughi, D. E. Starr, E. Handick, S. D. Stranks, M. Gorgoi, R. G. Wilks, M. Bär and H. J. Snaith, *ACS Appl. Mater. Interfaces*, 2015, **7**, 13440–13444.
16 D. Meggiolaro, S. G. Motti, E. Mosconi, A. J. Barker, J. Ball, C. A. R. Perini, F. Deschler, A. Petrozza and F. De Angelis, *Energy Environ. Sci.*, 2018, **11**, 702–713.

17 M. H. Du, *J. Mater. Chem. A*, 2014, **2**, 9091–9098.
18 W.-J. Yin, T. Shi and Y. Yan, *Adv. Mater.*, 2014, **26**, 4653–4658.
19 G. Nan, X. Zhang, M. Abdi-Jalebi, Z. Andaji-Garmaroudi, S. D. Stranks, G. Lu and D. Beljonne, *Adv. Energy Mater.*, 2018, **8**, 1702754.
20 J. VandeVondele, M. Krack, F. Mohamed, M. Parrinello, T. Chassaing and J. Hutter, *Comput. Phys. Commun.*, 2005, **167**, 103 – 128.
21 S. Goedecker, M. Teter and J. Hutter, *Phys. Rev. B*, 1996, **54**, 1703–1710.
22 J. VandeVondele and J. Hutter, *J. Chem. Phys.*, 2007, **127**, 114105.
23 J. Lahnsteiner, G. Kresse, A. Kumar, D. Sarma, C. Franchini and M. Bokdam, *Phys. Rev. B*, 2016, **94**, 214114.
24 Y. Kawamura, H. Mashiyama and K. Hasebe, *J. Phys. Soc. Jpn*, 2002, **71**, 1694–1697.
25 X.-Y. Zhu and V. Podzorov, *J. Phys. Chem. Lett.*, 2015, **6**, 4758–4761.
26 H. Zhu, K. Miyata, Y. Fu, J. Wang, P. P. Joshi, D. Niesner, K. W. Williams, S. Jin and X.-Y. Zhu, *Science*, 2016, **353**, 1409–1413.
27 K. Miyata, D. Meggiolaro, M. T. Trinh, P. P. Joshi, E. Mosconi, S. C. Jones, F. De Angelis and X.-Y. Zhu, *Sci. Adv.*, 2017, **3**, e1701217.
28 S. A. Bretschneider, I. Ivanov, H. I. Wang, K. Miyata, X. Zhu and M. Bonn, *Adv. Mater.*, 2018, 1707312.
29 F. Ambrosio, J. Wiktor, F. De Angelis and A. Pasquarello, *Energy Environ. Sci.*, 2018, **11**, 101–105.
30 J. P. Perdew, M. Ernzerhof and K. Burke, *J. Chem. Phys.*, 1996, **105**, 9982–9985.
31 L. D. Whalley, R. Crespo-Otero and A. Walsh, *ACS Energy Lett.*, 2017, **2**, 2713–2714.
32 M. Sprik and G. Ciccotti, *J. Chem. Phys.*, 1998, **109**, 7737–7744.
33 G. Ciccotti and M. Ferrario, *J. Mol. Liq.*, 2000, **89**, 1–18.
34 H. Flyvbjerg and H. G. Petersen, *J. Chem. Phys.*, 1989, **91**, 461–466.
35 A. Miyata, A. Mitioglu, P. Plochocka, O. Portugall, J. T.-W. Wang, S. D. Stranks, H. J. Snaith and R. J. Nicholas, *Nat. Phys.*, 2015, **11**, 582–587.
36 Q. Lin, A. Armin, R. C. R. Nagiri, P. L. Burn and P. Meredith, *Nat. Photonics*, 2015, **9**, 106.
37 J. Wiktor, U. Rothlisberger and A. Pasquarello, *J. Phys. Chem. Lett.*, 2017, **8**, 5507–5512.
38 W. Li, J. Liu, F.-Q. Bai, H.-X. Zhang and O. V. Prezhdo, *ACS Energy Lett.*, 2017, **2**, 1270–1278.